Spherically-Based Radon Transforms for Spotlight-Mode Synthetic Aperture Radar

Jordan Mann * Robert Hummel
Courant Institute of Mathematical Sciences
New York University

February 1993

Abstract

Spotlight-mode synthetic aperture radar (SAR), a method of imaging using radar, uses the assumption that the distance from the radar antenna to the region to be imaged is large in comparison to the size of the region, so that a wavefront striking the region may be said to lie approximately in a straight line (the intersection of two planar surfaces). Reconstruction is then based on the Radon Slice Theorem. The assumption places limits on the size of the region that can be imaged and on the resolution of the image.

The true wavefront of the radar signal is spherical, and intersects the planar or spherical imaging region in circles. An algorithm by Bauck[2] is similar to standard SAR imaging, but uses backprojection on circular arcs. Although there is no mathematical justification for the method other than analogy to the line-based backprojection method, Bauck's algorithm works well experimentally.

We show that if the imaging region resides on the surface of a sphere and the radar antenna orbits over a great circle on the sphere, then a simple projection of the sphere onto the plane transforms all the curved integration paths on the sphere to lines segments in the plane, allowing a minor modification of the backprojection algorithm to compute the image without distortion. We compare the resulting algorithm to one which assumes planar imaging regions and wavefronts.

1 Background

Synthetic Aperture Radar (SAR) is a method of making high-resolution maps of the earth or other planets using radar signals. It can be used to obtain geological or agricultural data or to monitor the movement of ice or oil slicks. It also has military and strategic applications. (For a more detailed listing, see [2]). The different types of SAR include strip-map, spotlight-mode, and inverse SAR. This paper will focus on spotlight-mode.

The classical approach to spotlight-mode SAR image reconstruction can be formulated as an analogue to computed tomography [5]. Every point in the ground patch to be imaged is assumed to have a numerical radar reflectivity value. Information about the radar reflectivity of the various

*This work forms a portion of the PhD dissertation of Jordan Mann.

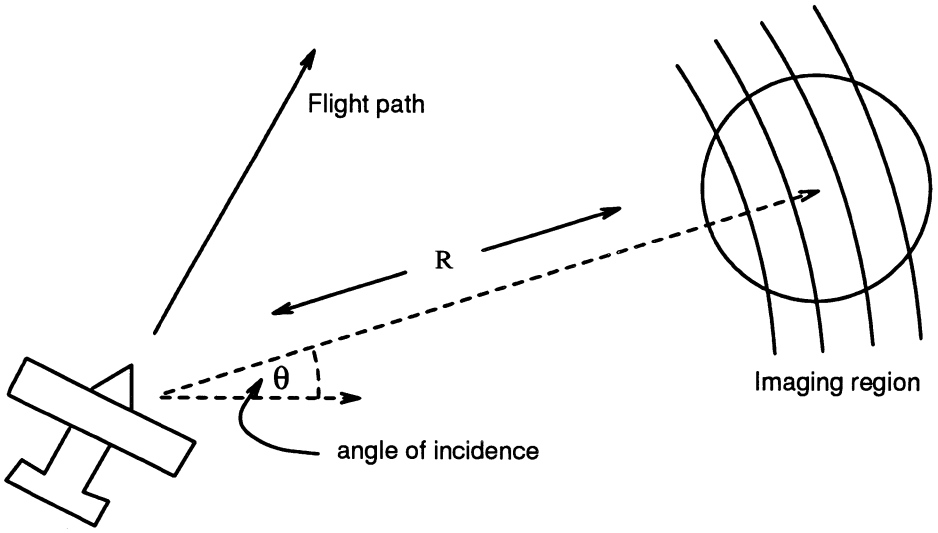

Figure 1: The classical SAR geometry. Since the extent of the ground patch is much smaller than R, the distance of the radar antenna from the center of the ground patch, any arc along which the spherical wavefront intersects the ground patch can be approximated by the straight line $x\cos\theta + y\sin\theta = \sigma$ for some value of σ.

points in the ground patch is gathered by broadcasting a radar signal at the ground patch from a series of distant positions. From each position, the amplitude of the returning signal is measured as a function of time. It is assumed that the ground patch is distant from the radar antenna, and thus the wavefronts striking the ground patch are approximately planar, and the intersections of the wavefronts with the flat ground patch lie approximately in straight lines. The response to a delta pulse from the antenna will be a return signal whose value at any given instant is proportional to the integral of the reflectivity along one such straight line (see Figure 1).

Let us recall the definition of the Radon transform. Given a function $g(x, y)$, the Radon transform of g at angle θ and position σ, denoted $P_\theta g(\sigma)$, is given by

$$P_\theta f(\sigma) = \int_{-\infty}^{\infty} f(\sigma\cos\theta - \tau\sin\theta, \sigma\sin\theta + \tau\cos\theta)\, d\tau. \tag{1}$$

Put differently, $P_\theta g(\sigma)$ is the integral of g along the line $x\cos\theta + y\sin\theta = \sigma$ in the x-y plane (see Figure 1). If the radar reflectivity of a point (x, y) in the ground patch is given by the function $g(x, y)$, then $P_\theta g(\sigma)$ for various values of θ and σ may be determined from the reflected signal data.

Suppose that the antenna transmits a signal $s(t)$. It can be argued by superposition that the return signal $r(t)$ is essentially the convolution of $P_\theta g$, the Radon transform of the reflectivity for a particular angle θ, with the transmitted signal $s(t)$ (see [5]). It is desired to obtain the Fourier transform of $P_\theta g$; this could be done by dividing the Fourier transform of the return signal by that of the transmitted signal (since the Fourier transform of the convolution of two functions is

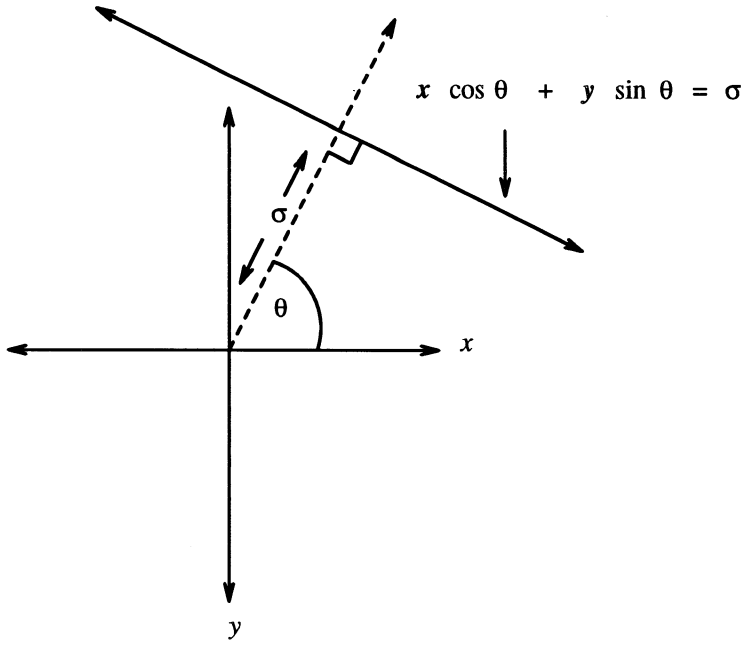

Figure 2: The Radon transform of f at angle θ and position σ, denoted $P_\theta f(\sigma)$, is the integral of f on the line $x\cos\theta + y\sin\theta = \sigma$.

---

the product of their Fourier transforms), but other signal processing techniques are usually used instead [5].

By determining $\widehat{P_\theta g}(\rho)$, the Fourier transform of the Radon transform for a particular angle (i.e., the Fourier tranform of $P_\theta g$ taken with respect to the position variable σ but not with respect to the angle θ), one actually determines the Fourier transform of g itself, thanks to the Radon Slice Theorem (see [5]):

$$\widehat{P_\theta g}(\rho) = \sqrt{2\pi}\hat{g}(\rho\cos\theta, \rho\sin\theta). \tag{2}$$

In other words, the values of $\widehat{P_\theta g}$ are proportional to those of $\hat{g}$ on a line in the spectral plane which forms an angle θ with the horizontal axis. By computing $\widehat{P_\theta g}(\rho)$ for various values of ρ and θ, one obtains the values of $\hat{g}$ on a polar grid in the spectral domain. Traditionally, the values of $\hat{g}$ on a rectangular grid are then determined by interpolation from those on the polar grid, although the tomographic formulation shows that the backprojection algorithm used in computed tomography may be used instead (see [3]).

2 Limitations of conventional SAR geometric assumptions

In reality, of course, the wavefronts striking the patch lie more nearly in a spherical surface than a planar one, and do not intersect the ground patch in straight lines. Consequently, limits must be placed on the dimensions of the physical system in order that the assumptions be "approximately" correct. In [5] it is shown that range resolution (resolution in the direction of travel of the radar

signal) can be no smaller than

$$\frac{L^2}{R},$$

for otherwise the wavefront curvature will cause some points to contribute information to the wrong resolution box. It is also shown in [5] that in order to preserve the coherence of the return signal, it is necessary that

$$\frac{L^2 \sin 2\theta_M}{4R} \ll \frac{\lambda}{8},$$

where θ_M is the range of angles at which radar signals are transmitted and λ is the wavelength associated with the primary frequency of the signal.

3 Hemisphere reconstruction method

As a result, it is desirable to develop reconstruction algorithms that work with integrals of the image function along circular arcs instead of straight lines. Clearly, algebraic reconstruction techniques (such as the one presented in [2,1] will be as effective for the arc case as they are for the straight-line case, but these techniques are slow compared to Fourier-based techniques and therefore are not used often.

We will instead propose the hemisphere reconstruction method, which eliminates the approximation of arcs by straight lines while simultaneously eliminating another approximation, that of the surface of the earth (or planet) by a plane. The method will assume the planet is a sphere, and that the radar antenna is located above the planet. In this algorithm, the unknown reflection function g lies on a patch on the hemisphere

$$H = \{(x, y, z) : x^2 + y^2 + z^2 = 1, z > 0\},$$

and the result of the radar emissions and signal processing will be that the integrals of g along arcs will be known. However, because there is no suitable Fourier decompostion of g, which is supported on H, our algorithm projects the problem onto the plane, and recovers g by solving a Radon projection problem in the plane.

3.1 Formulation of the problem

In this subsection, we formulate the reconstruction problem through examination of the three-dimensional SAR geometry. In the next subsection, we provide the algorithmic solution.

We begin by recalling the situation in the plane. If $f(x, y)$ is a reflection function defined on $\mathbf{R}^2$, supported on a compact patch, then a radar "chirp" $s(t)$ emitted from a distant point $(-R\cos\theta, -R\sin\theta)$ will yield a response

$$r_\theta(t) = \int P_\theta(l - R)\, s\left(t - \frac{2l}{c}\right) dl,$$

as explained in [5]. The Radon transform $P_\theta f$, defined in (1), can also be written

$$P_\theta f(\sigma) = \int_{l_\theta(\sigma)} f\, dl, \tag{3}$$

where $l_\theta(\sigma)$ is the line

$$l_\theta(\sigma) = \{x\cos\theta + y\sin\theta = \sigma\}$$

and dl is the arc length measure.

For a function $g(x,y,z)$ supported on the hemisphere H, let us suppose that a chirp $s(t)$ is emitted from a point $(-R\cos\theta, -R\sin\theta, 0)$, which is directly "above" the hemisphere's "equator", which is the set of points $(x,y,z) \in H$ such that $z = 0$. We will use the following notation for a certain set of arcs on H. Let

$$P_\theta(\sigma) = \{(x,y,z) : x\cos\theta + y\sin\theta = \sigma\},$$

which is a plane perpendicular to the x-y plane, and let

$$l_\theta(\sigma) = P_\theta(\sigma) \cap H.$$

Thus $l_\theta(\sigma)$ is the arc across H that lies in a vertical plane normal to the θ direction, lying σ units from the origin. It is easy to check that the distance $d_A(x,y,z)$ from the antenna of any point on H is given by

$$d_A(x,y,z) = d_s(x\cos\theta + y\sin\theta),$$

where

$$d_s(\sigma) = \sqrt{1 - 2R\sigma + R^2}. \tag{4}$$

Thus d_A is constant on $l_\theta(\sigma)$. The arcs $\{l_\theta(\sigma)\}$, for varying θ and σ, will be the curves along which the integral of g will be known. See Figure 3.

Specifically, let

$$Q_\theta(\sigma) = \frac{1}{\sqrt{1-\sigma^2}} \int_{l_\theta(\sigma)} g\, dl,$$

by rough analogy to the Radon transform as defined in (3). Explicitly,

$$Q_\theta(\sigma) = \int_{\mathbf{R}} \frac{g(\sigma\cos\theta - \tau\sin\theta, \sigma\sin\theta + \tau\cos\theta, \sqrt{1-\sigma^2-\tau^2})}{\sqrt{1-\sigma^2-\tau^2}}\, d\tau. \tag{5}$$

These integrals can be extracted by deconvolution from the return signal, since

$$r_\theta(t) = \int_{-1}^{1} Q_\theta(\sigma)\, s\left(t - \frac{2d_s(\sigma)}{c}\right), \tag{6}$$

where c is the speed of light, as we will know show.

We will make two assumptions common to all SAR reconstruction algorithms, namely, that radar reflectivity is independent of the direction from which the signal strikes the object and that the radar reflectivity function g vanishes outside a ground patch on the hemisphere, which is equivalent to assuming that if the antenna illuminates any portion of the sphere outside the ground patch, then the strength of the signal reflected from that portion is negligible.

Let $g(x,y,z)$ be the radar reflectivity function, defined for any coordinate triplet (x,y,z) located on H. Again, let $s(t)$ denote the amplitude of the transmitted signal at time t. As before, we note that the amplitude of the signal reflected from a point (x,y,z) in the ground patch to the antenna at time t is given by

$$g(x,y,z)\, s\left(t - \frac{2d_A(x,y,z)}{c}\right),$$

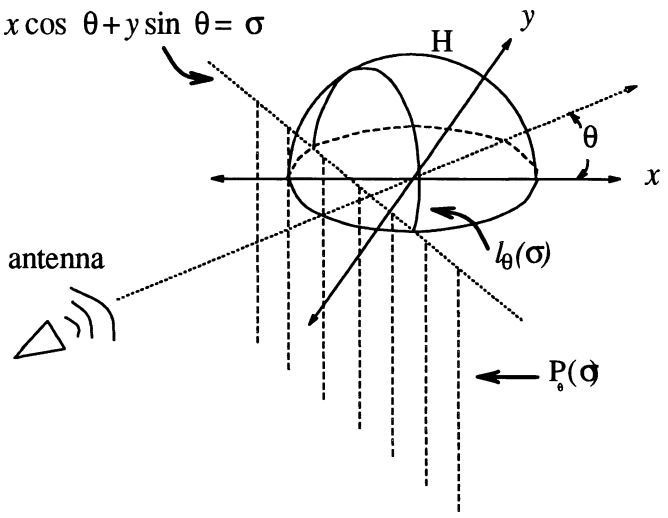

Figure 3: Spherical SAR geometry.
The antenna broadcasts a signal from a point $(-R\cos\theta, -R\sin\theta)$ toward the hemisphere H. The arc $l_\theta(\sigma)$ is the set of points on H whose coordinate in the θ direction is σ. It lies in the vertical plane $P_\theta(\sigma)$ and is above the line $\{x\cos\theta + y\sin\theta = \sigma, z > 0\}$. Points on $l_\theta(\sigma)$ are equidistant from the antenna.

---

where $d_A(x,y,z)$ is the distance of the point (x,y,z) from the antenna. It follows that $r(t)$, the total signal reflected to the antenna from the ground patch at time t, is given by

$$r_\theta(t) = \int_H g(x,y,z)\, s\left(t - \frac{2d_P(x,y,z)}{c}\right) dS,$$

where dS indicates the surface area integral. Since

$$d_A(x,y,z) = d_s(x\cos\theta + y\sin\theta),$$

we may make the following change of variable in order to simplify the last integral:

$$\begin{aligned} \sigma &= x\cos\theta + y\sin\theta \\ \tau &= -x\sin\theta + y\cos\theta \end{aligned}.$$

Then the last integral may be written

$$\begin{aligned} & r(t) \\ &= \int_{-1}^{1}\int_{-\sqrt{1-\sigma^2}}^{\sqrt{1-\sigma^2}} g(\sigma\cos\theta - \tau\sin\theta, \sigma\sin\theta + \tau\cos\theta, \sqrt{1-\sigma^2-\tau^2}) \\ &\qquad \cdot s\left(t - \frac{2d_s(\sigma)}{c}\right) \frac{d\tau\, d\sigma}{\sqrt{1-\sigma^2-\tau^2}} \\ &= \int_{-1}^{1} Q_\theta(\sigma)\, s\left(t - \frac{2d_s(\sigma)}{c}\right) d\sigma. \end{aligned}$$

Thus Equation (6) is proved.

3.2 Derivation of the algorithm

In deriving the Hemisphere reconstruction algorithm, we will first show how to extract the normalized integrals $Q_\theta g(\sigma)$ from the return signal. We will then show that the $Q_\theta g$ are in fact the Radon transforms of a function $\tilde{g}$ defined in the horizontal plane. Thus the $Q_\theta g$ allow reconstruction of $\tilde{g}$. Finally, we show that g is easily determined from $\tilde{g}$.

First, the extraction of $Q_\theta g$ from the return signal. Let

$$\tau(\sigma) = \frac{2d_s(\sigma)}{c}. \tag{7}$$

which is the roundtrip travel time of the radar signal between the antenna and a point on $l_\theta(\sigma)$. Solving for σ, we find that

$$\sigma(\tau) = \frac{4R^2 + 4 - c^2\tau^2}{8R} \tag{8}$$

and therefore we obtain $d\sigma = -\frac{c^2}{4R}\tau\, d\tau$. Changing variables in (6), we may write

$$r(t) = \frac{c^2}{4R}\int_{-\infty}^{\infty} G_\theta(\tau)\, s(t-\tau)\, d\tau,$$

where

$$G_\theta(\tau) = \tau Q_\theta(\sigma(\tau)) \tag{9}$$

and $G_\theta(\tau)$ vanishes for $\tau \notin [\tau(1), \tau(-1)]$. Thus G_θ can be obtained from the return signal by deconvolution, since s is known. Then $Q_\theta g$ can be obtained by means of

$$Q_\theta g(\sigma) = \frac{G_\theta(\tau(\sigma))}{\tau(\sigma)}. \tag{10}$$

Thus the $Q_\theta g$ can be obtained by deconvolution from the return signal.

We know show that the $Q_\theta g$ are the Radon transforms of a function $\tilde{g}$ defined in the plane. Specifically, let

$$\tilde{g}(x,y) = \frac{g(x,y,\sqrt{1-x^2-y^2})}{\sqrt{1-x^2-y^2}}, \qquad x^2+y^2<1, \tag{11}$$

and $\tilde{g} = 0$ for $x^2 + y^2 \geq 1$. Using the definition of the Radon transform given by Equation (1), the definition of $Q_\theta g$ given by (5), and the fact that for any θ,

$$(\sigma\cos\theta - \tau\sin\theta)^2 + (\sigma\sin\theta + \tau\cos\theta)^2 = \sigma^2 + \tau^2,$$

it is easy to show that

$$Q_\theta g(\sigma) = P_\theta \tilde{g}(\sigma). \tag{12}$$

Since the Radon transform data of $\tilde{g}$ is known, the convolution backprojection algorithm, or any other algorithm for reconstruction from Radon transforms, may be used to compute $\tilde{g}$. Finally, we see from (11) that g is easily reconstructed using the relationship

$$g(x,y,\sqrt{1-x^2-y^2}) = \tilde{g}(x,y)\sqrt{1-x^2-y^2}.$$

3.3 Summary of the algorithm

We have thus derived the following algorithm:

Let $(R_1, \theta_1), \ldots, (R_N, \theta_N)$ be the set of points in the x-y plane, specified by polar coordinates, from which radar signals are broadcast. For $i = 1 \ldots N$, do the following:

1. Broadcast the radar signal, remove the transmitted signal $s(t)$ from the reflected signal $r(t)$ by deconvolution, and divide by $c^2/4R_i$, where c is the speed of light, in order to obtain $G_{\theta_i}(\tau)$.
2. Following (4) and (7), Let
$$\tau^i(\sigma) = \frac{2\sqrt{1 - 2\sigma R_i + R^2}}{c}.$$
3. Following (10), let
$$Q_{\theta_i}(\sigma) = \frac{G_{\theta_i}(\tau^i(\sigma))}{\tau^i(\sigma)}.$$
By (12), this equals $P_{\theta_i}\tilde{g}(x)$.

Reconstruct $\tilde{g}$ from its Radon transforms $P_{\theta_i}\tilde{g}(x)$, using any known algorithm, and finally reconstruct g using
$$g(x, y, \sqrt{1 - x^2 - y^2}) = \tilde{g}(x, y)\sqrt{1 - x^2 - y^2},$$
as indicated above.

We note again that the algorithm is designed for data resident on a sphere, and dispenses with the approximation of regions on spheres by planes which is necessary for conventionaly SAR processing. The method requires that the antenna path lie in a plane containing the center of the sphere, which we assumed in our exposition, without loss of generality, to be the x-y plane.

3.4 Further geometric consideratations

The algorithm is motivated by the geometric observation that g is transformed into $\tilde{g}$ by "flattening" the hemisphere H onto the x-y plane, in the following sense. If we map every point $(x, y, \sqrt{1 - x^2 - y^2})$ in H onto the point $(x, y, 0)$ which is directly below it, then H is mapped to the disk
$$\{(x, y, z) : x^2 + y^2 < 1,\ z = 0\},$$
and the arc $l_\theta(\sigma)$ is mapped to a segment of the line
$$x \cos\theta + y \sin\theta = \sigma.$$

As (11) makes clear, the value of $\tilde{g}$ at a point (x, y) depends on the value of g at the point on H which is mapped to $(x, y, 0)$ by this flattening.

3.5 other considerations

We note that it is easy to compensate for signal attenuation using this algorithm. Attenuation of the amplitude of the signal reflected from a point (x, y, z) is proportional to the inverse square of the distance of (x, y, z) from the antenna. Since τ, the variable introduced in our derivation of the algorithm, is proportional to this distance, as stated earlier, it follows that amplitude attenuation is proportional to τ^{-2}, and one can compensate for the attenuation by multiplying $G_\theta(\tau)$ by a constant times τ^2 before further processing.

Of course, it is impractical in many situations to have an SAR antenna traverse a great circle route, or even half of a great circle route, as the hemisphere reconstruction method would require. However, the Radon Slice Theorem, as used in standard SAR image reconstruction, theoretically requires a full 180° viewing angle, and yet in practice, quality images are obtained from a viewing angle as small as 6°. (For a discussion of why this is so, see [6].) It is hoped that this algorithm would obtain better results using a few degrees of the earth's circumference, which is a few hundred miles. In situations where this too is impractical, it may be possible to fly a shorter distance along one great circle and then turn and fly along a different great circle, and to combine the two resulting images. This has not yet been explored.

4 Experimental Results

4.1 Choice of function

The hemisphere reconstruction method, and an algorithm employing the planar wavefront and flat ground patch assumptions, which we will call "the plane algorithm", were used to reconstruct a function g defined on the hemisphere

$$H = \{(x, y, z) : x^2 + y^2 + z^2 = 1, z > 0\},$$

and the resulting images are shown. The function g is defined by

$$g(x, y, z) = 0.95\, I_A(x, y, z) - 0.2\, I_B(x, y, z) + 0.5\, I_C(x, y, z) + 0.7\, I_D(x, y, z),$$

where $I_A, \ldots, I_D$ are the indicator functions respectively of the sets

$$A = \{(x, y, z) \in H : 4(x - 0.375)^2 + (y - 0.25)^2 < 0.25$$

$$B = \{(x, y, z) \in H : 9(x - 0.375)^2 + 4(y - 0.4375)^2 < 0.140625$$

$$C = \{(x, y, z) \in H : (x - 0.75)^2 + y^2 < 0.008789$$

$$D = \{(x, y, z) \in H : (x - 0.25)^2 + (y + 0.5)^2 < 0.015625.$$

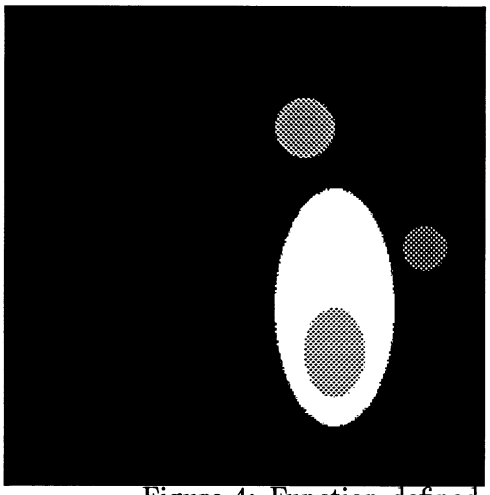

Figure 4: Function defined on the hemisphere.
This image may be thought of as a view of the hemisphere from $+\infty$ on the z-axis. I.e., to create this 2-D image, the hemisphere has been "flattened" by mapping every point (x, y, z) on the hemisphere to $(x, y, 0)$.

4.2 Distortion associated with assumption of planar geometry

Our implementation of the plane algorithm incorporates the distortions that result when the plane algorithm is applied to signals reflected from a sphere. These distortions were determined as follows. The plane algorithm assumes that the ground patch lies in horizontal plane and that the antenna is above it. We may assume here that a coordinate system $(\overline{x}, \overline{y})$ is chosen in such a way that the antenna lies above the point $(R_p, 0)$, for some $R_p > 0$, at a height h above the plane. The algorithm also makes the familiar assumption that for any point $(\overline{x}, \overline{y})$ in the ground patch, $\overline{x}^2 + \overline{y}^2 \ll R_p^2$, and thus the distance of the point from the antenna position depends only on $\overline{x}$. We may say that the distance of $(\overline{x}, \overline{y})$ from the point $(R_p, 0)$ is $R_p - \overline{x}$, and thus the distance of $(\overline{x}, \overline{y})$ from the antenna is given by $\sqrt{(R_p - \overline{x})^2 + h^2}$. Then, using an analysis similar to the one in the previous section, we conclude that $r(t)$, the return signal at time t, equals

$$\frac{c^2}{2} \int G^p(\tau) s(t - \tau)\, d\tau$$

where

$$G^p(\tau) = \frac{\tau P_0 g(\overline{x}(\tau))}{\sqrt{c^2\tau^2 - 4h^2}}, \tag{13}$$

$$\overline{x}(\tau) = R_p - \sqrt{\frac{c^2}{4}\tau^2 - h^2}, \tag{14}$$

and $P_0 g$ is the Radon transform of the reflectivity function g at angle 0. G^p is obtained by deconvolution, and then $P_0 g$ is obtained by solving for $P_0 g$ in (13). Substituting (7) in (14), we find that when the plane algorithm is applied to signals reflected from a sphere, data that should be associated with the horizontal position x are in fact associated with the horizontal position

$$\overline{x} = R_p - \sqrt{1 - 2xR + R^2 - h^2}, \tag{15}$$

where R is the actual distance of the antenna from the center of the sphere. Further distortion in the application of the plane algorithm to such signals results from the fact that while the deconvolved signal $G(\tau)$ should be divided by τ, as in (10), to obtain the Radon transform, the plane algorithm divides the deconvolved signal (which we have referred to in (13), in the context of the plane algorithm, as G^p) by $\tau/\sqrt{c^2\tau^2 - 4h^2}$. Also, while the result of the (correct) division is $P_0\tilde{g}$, the Radon transform of $\tilde{g}$, which is given by (11), the plane algorithm treats the result of this division as $P_0 g$. In summary, the plane algorithm sets $P_0 g(\overline{x})$ equal to

$$\sqrt{c^2\tau^2 - 4h^2} P_0\tilde{g}(x(\overline{x})),$$

where $x(\overline{x})$ is obtained by solving for x in (15). It follows that for any θ, the plane algorithm sets $P_\theta g(\overline{x})$ equal to

$$\sqrt{c^2\tau^2 - 4h^2} P_\theta\tilde{g}(x(\overline{x})). \tag{16}$$

(Actually, the conventional implementation of the plane algorithm uses a linear approximation of the right side of (14) to compute $\overline{x}$, as shown in [5], but the resulting relationship between the true horizontal coordinate x and the computed coordinate $\overline{x}$ will be of the same form as (15), and it is reasonable to assume that in situations where there is a significant discrepancy between the right side of (14) and the linear approximation, the linear approximation will make the distortion worse, not better.)

4.3 Implementation of hemisphere and plane algorithms

In our numerical experiment, we first computed $P_\theta\tilde{g}$ numerically, from its definition (see (11) and (1)), for all θ in $\{0, \pi/40, 2\pi/40, \ldots, 39\pi/40\}$. Our implementation of the hemisphere reconstruction method reconstructed $\tilde{g}$ from the $P_\theta\tilde{g}$ using the convolution-backprojection method, and then multiplied by $\sqrt{1 - x^2 - y^2}$ to obtain g. In our implementation of the plane algorithm, for every value of $\overline{x}$ in $\{-1, -511/512, -510/512, \ldots, 511/512\}$, $x(\overline{x})$ was computed by solving for x in (15), $P_\theta\tilde{g}(x(\overline{x}))$ was computed numerically, and $P_\theta g(\overline{x})$ was set equal to

$$\sqrt{c^2\tau^2 - 4h^2} P_\theta\tilde{g}(x(\overline{x})),$$

with τ defined as in (7) and R, R_p, and h defined below. The reflectivity function g was then computed from the $P_\theta g(\overline{x})$ using the convolution-backprojection method, and was not multiplied by $\sqrt{1 - x^2 - y^2}$. The results are shown in Figure 5. (Of course, in reality, the plane algorithm is used quite often, and provides images far better than the one we present here. This is because it is applied to ground patches which are small with respect to their distances from the antenna and the radii of the spheres on which they lie. In our case, we have used the plane algorithm on a ground patch which is large with respect to these distances. The advantage of using the hemisphere algorithm is much more evident on such a ground patch.)

For the purposes of our implementation of the plane algorithm, it was assumed that the antenna "actually" traveled in the circle

$$x^2 + y^2 = R^2 = (1.5)^2$$

in the x-y plane, bouncing signals off the hemisphere H. The plane algorithm "pretended" that the ground patch lay in a plane and that the height h of the antenna above this plane was 0.5, which was the "actual" distance of the antenna from the hemisphere, and assumed that the antenna was

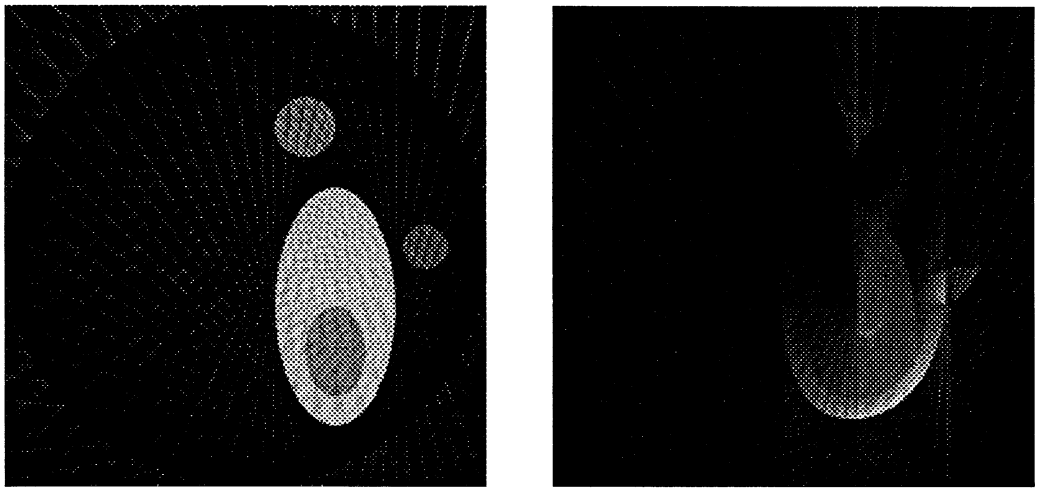

Figure 5: Reconstructions of the function.
On the left, result of spherical algorithm; on the right, result of plane algorithm. For both images, the hemisphere was "flattened" in the manner described in the previous caption.

---

over a point in the plane which was a distance $R_p = \pi/2$ from the origin, since the antenna was "actually" flying over the circle $x^2 + y^2 = 1$ on the hemisphere, and all points on this circle lie an arc length distance of $\pi/2$ from the top of the hemisphere (the point $(0, 0, 1)$).

References

[1] J.L. Bauck, W.K. Jenkins, "Tomographic processing of spotlight-mode synthetic aperture radar signals with compensation for wavefront curvature," *Proceedings of the IEEE International Conference on Acoustics, Speech, and Signal Processing*, New York, pp. 1192–1195, April 1988.

[2] J.L. Bauck, "Tomographic processing of synthetic aperture radar signals for enhanced resolution," Ph.D. dissertation, Univ. of Illinois, 1990.

[3] M.D. Desai, W.K. Jenkins, "Convolution backprojection image reconstruction for spotlight mode synthetic aperture radar," *IEEE Transactions on Image Processing*, vol. 1, no. 4, Oct. 1992, pp. 505–517.

[4] G.T. Herman, *Image Reconstruction from Projections: The Fundamentals of Computerized Tomography.* New York: Academic Press, 1980.

[5] D.C. Munson, Jr., J.D. O'Brien, W.K. Jenkins, "A tomographic formulation of spotlight-mode synthetic aperture radar," *Proceedings of the IEEE*, vol. 71, no. 8, Aug. 1983, pp. 917–925.

[6] D.C. Munson, Jr. and J.L.C. Sanz, "Image reconstruction from frequency-offset Fourier data," *Proceedings of the IEEE*, vol. 72, no. 6, June 1984, pp. 661-669.